Generalization Approach for Models of Thermal Buffer Storages in Predictive Control Strategies

Julian Buderus, Arno Dentel
Technische Hochschule Nuernberg Georg Simon Ohm, Nuremberg, Germany

Abstract

The demand for flexibility in a future electricity system, mainly based on renewable energies, will increase. Flexible building devices combined with predictive control strategies can help to cover this increasing demand for flexibility. Predictive control strategies allow an optimization of the operation mode of e.g. heat pumps or combined heat and power units with a regard to the current availability of electricity in the power grid. With thermal storage units, the available flexibility of the thermal generation units increases and avoids influences on the thermal comfort in the building. For an optimized operation, a supervisory control has to be equipped with models of the building devices and the storage units. Those models have to be as simple as possible to reduce computation time as well as the effort during the commissioning process.

This paper describes a generalization approach for a model of thermal buffer storages. The generalized model is derived from a detailed model, developed in Dymola, and is based on characteristic curves, which describe the temperature of the storage medium depending on the current state of charge. The developed models are validated using measurement data from a hardware test bench. The results of the validation show, that the deviation of the simulated storage temperature are between 5 and 22 %, depending on the observed temperature layer in the current operation mode (loading or unloading).

Introduction

To reduce the energy-related greenhouse gas emissions many countries are working on the transformation of their energy system. The reduced dependency on energy imports is also a driving factor for local power generation. Today the new installation capacity of renewable energy sources, like wind and solar power, exceeds the one from fossil fuels REN21 (2016). However, the uncontrollable generation of many renewable energy sources (e.g. wind and photovoltaic) requires compensation mechanisms to enable a stable operation of the power grid. Arteconi et al. (2013) analyses the potential of heat pumps (HP-Units) combined with thermal energy storages (TES) for a domestic demand-side-management. The developed operation strategy reduces the electrical power demand of the HP-Unit during peak hours. In combination with a flexible energy tariff, a reduction of energy costs would also be possible. Widmann et al. (2017) describes an operation strategy for combined heat and power units (CHP-Units) and TES to increase the in-house power consumption. This strategy is tested in simulation studies and with a real plant and leads to a higher in-house consumption by using a smart management of the TES. For the implementation of a predictive control strategy, models of the technical devices are necessary to be used for the optimization and planning process. Becker (2006) presents a detailed model of a thermal buffer storage, which allows the simulation of the density dependent stratification in the storage. However, for the use in a predictive control strategy, the models have to be simple and easy to parameterize to reduce computation time and enable an easy commissioning process. This paper describes a generalization approach for thermal buffer storage units. The generalized model is derived from a detailed model developed in Dymola from Dassault Systemes (2016) and utilizes characteristic curves to determine the temperature distribution inside the storage unit. The developed models are validated with measurement data from a hardware test bench.

Modelling

In a first step, a detailed model of a thermal buffer storage unit is developed. The model is based on the work of Becker (2006) and represents a stratified storage with configurable number of layers. The model is developed in the software environment Dymola. The library TIL Media developed by TLK Thermo GmbH (2016) allows the implementation of the physical substance data of the specific storage medium. The differential equation, which is used for the calculation of the temperature of a certain storage layer is shown in (1).

$$\dot{\vartheta}_i = C \cdot (\sum \dot{Q}_{conv} + \sum \dot{Q}_{cond} + \\ + \sum \dot{Q}_{mix} + \sum \dot{Q}_{losses}). \quad (1)$$

with:

$$C = \left(\frac{V_{storage,total}}{k} \cdot \varrho_{water} \cdot c_{p,water} \right)^{-1} . \qquad (2)$$

The heat flows resulting from loading and unloading of the storage are represented by the variable $\dot{Q}_{conv}$. As the storage is divided in different thermal layers, heat conduction between the layers takes place ($\dot{Q}_{cond}$). In addition, losses to the environment are considered by $\dot{Q}_{losses}$. The losses to the environment are calculated for each layer by using the heat transfer coefficient of the insulation as well as the suface of the specific layer. To model the temperature-dependent density difference, the heat flow $\dot{Q}_{mixing}$ is defined. If the temperature above is lower than the temperature of the observed layer, a compensation stream with a fixed mass flow rate $\dot{m}_{mix}$ is supposed. Figure 1 shows the thermal heat flows for the i-th layer of the storage model.

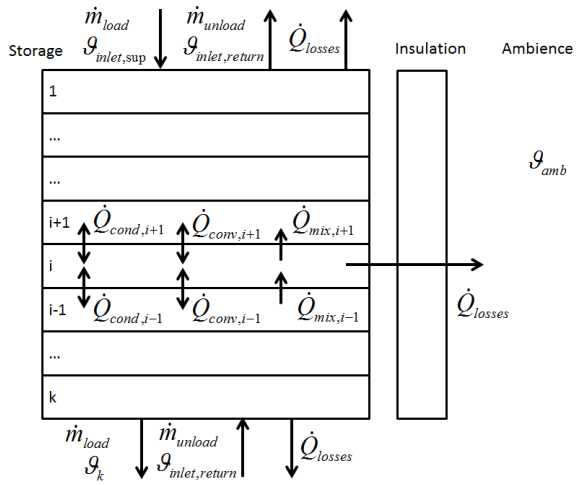

Figure 1: Heat flows in detailed buffer storage model (adapted from Becker (2006)).

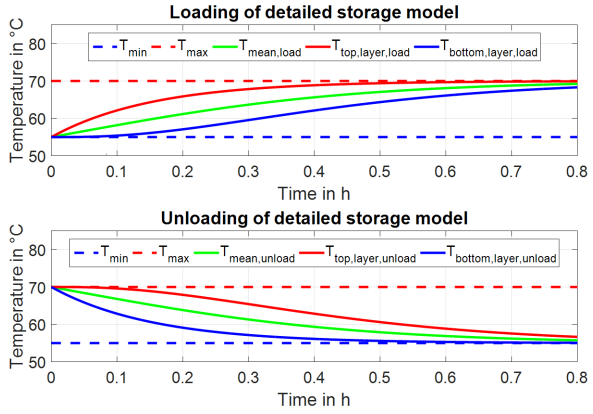

Figure 2: Loading and unloading of detailed storage model.

The model allows the configuration of geometrical properties (e.g. storage volume, height, etc.) as well as physical properties (e.g. heat transition coefficient of the insulation, specific heat capacity of the storage medium, etc.) of the specific storage unit. The inlet and outlet ports for the loading and unloading of the storage are located in the top and the bottom layer of the model. For the derivation of the generalized model, a loading and unloading process of the detailed model with three layers is observed. Figure 2 shows the resulting temperatures during the simulations. The temperature of the entering fluid is set constantly to 70 °C during loading and 55 °C during unloading. The mass flow rates are constant at 0.5 kg/s. For a first validation of the detailed model the TESS Type534 (Thermal Energy System Specialists (2012)) in TRNSYS (Solar Energy Laboratory (2012)) is used. The validation with the TESS model allows simple testing whether the developed model produces comprehensible results, without additional measurement data. Therefore, the same geometrical data, the same mass flow rates, the same number of layers as well as the same inlet temperature during loading and unloading are used. Figure 3 shows the results of the two simulation models and proofs that the developed model in Dymola shows a good accordance to the TESS model.

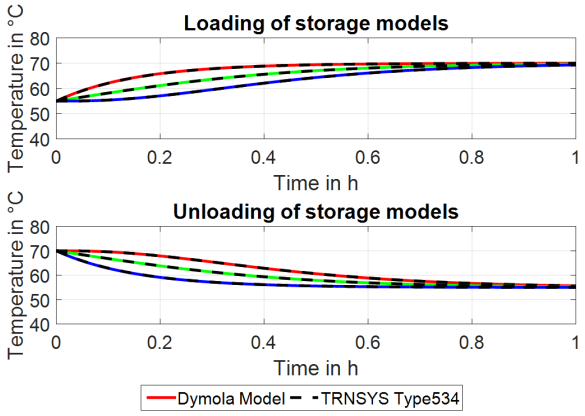

Figure 3: Loading and unloading of detailed storage model.

For the generalization approach of the model, characteristic curves are derived from the simulation data of the detailed model. The characteristic curves describe the temperature of a specific storage layer as a function of the current state of charge of the storage. Therefore, the temperatures of the top and the bottom layer are examined as well as the mean temperature. Since the procedure for the top and the bottom layer is the same, only the derivation of the characteristic curve of the top layer is presented.
Figure 4 visualizes the temperature of the top layer during loading and unloading of the storage as a function of the state of charge. The simulation results show, that the temperature curve during loading derivates from the temperature curve during unloading. The deviation is caused by the different inflows

during loading and unloading. For further work, the mean temperature of both will be used; the black solid line in figure 4 represents it.

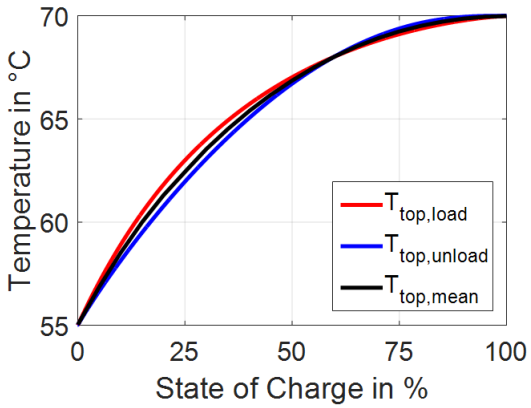

Figure 4: Temperature of top layer of detailed storage model.

With equation (3) the temperature of a specific layer is determined as a function of the state of charge (SOC). The temperatures ϑ_{min} and ϑ_{max} are constants and represent the minimum and maximum temperature of the specific heating system (e.g. 55/70 °C).

$$\vartheta_{layer}(t) = \vartheta_{min} + (p_1 \cdot SOC(t)^2 + \\ + p_2 \cdot SOC(t) + p_3) \cdot (\vartheta_{max} - \vartheta_{min}). \quad (3)$$

The coefficients (p_n) in equation (3) are results of the least squares method in MATLAB (Math Works (2015)). To model the temperature curve with a quadratic function as shown in equation (3), four sets of coefficients are necessary to reach a satisfactory accuracy. In figure 5 the solid lines (red, green, blue and yellow) visualize the results of equation (3) with different sets of coefficients.

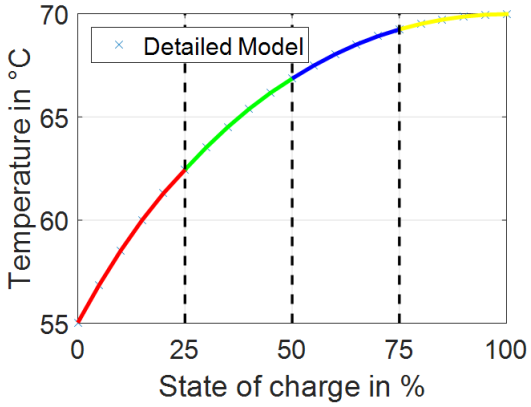

Figure 5: Mean temperature of top layer calculated with characteristic curves.

To model the mean temperature of the storage the fol-lowing equation is used:

$$\vartheta_{mean}(t) = \vartheta_{min} + (p_1 \cdot SOC(t) + p_2) \cdot \\ \cdot (\vartheta_{max} - \vartheta_{min}). \quad (4)$$

The mean temperature of the storage shows a linear behavior. Therefore, equation (4) has no square part and there is only one set of parameters necessary over the complete SOC of the storage. Figure 6 shows the results of the detailed model (x) and the characteristic curve (solid red line).

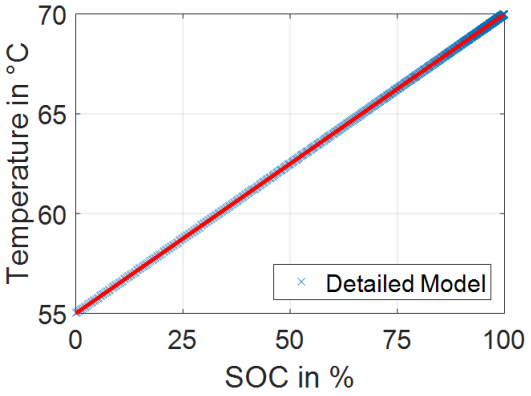

Figure 6: Mean temperature of storage calculated with characteristic curves.

The resulting coefficients for the top and bottom layer temperature as well as for the mean temperature are shown in the tables 1 - 3.

Table 1: Coefficients for top layer temperature.

SOC in %	p_1	p_2	p_3
0 - 25	-2.335	2.559	0.002
25 - 50	-1.344	2.184	0.035
50 - 75	-0.976	1.855	0.107
75 - 100	-0.772	1.548	0.223

Table 2: Coefficients for bottom layer temperature.

SOC in %	p_1	p_2	p_3
0 - 25	0.779	-0.001	0.001
25 - 50	0.485	0.252	-0.040
50 - 75	0.984	-0.082	0.007
75 - 100	2.238	-1.935	0.696

Table 3: Coefficients for mean temperature.

SOC in %	p_1	p_2
0 - 100	1	0

In the next step, loading and unloading procedures are simulated with the detailed model in Dymola. Afterwards the same loading and unloading conditions are used as inputs for the generalized model to compare the results. The storage is completely mixed at the beginning of the simulation and has a temperature of 70 °C. This state is defined as fully charged with a SOC of 100 %. The storage is unloaded for 2500 s with a constant mass flow rate of 0.5 kg/s and a constant unloading temperature of 55 °C. After a short delay, the loading process starts with the same mass flow rate but an inlet temperature of 70 °C. Figure 7 visualizes the temperatures and the calculated SOC of the two models.

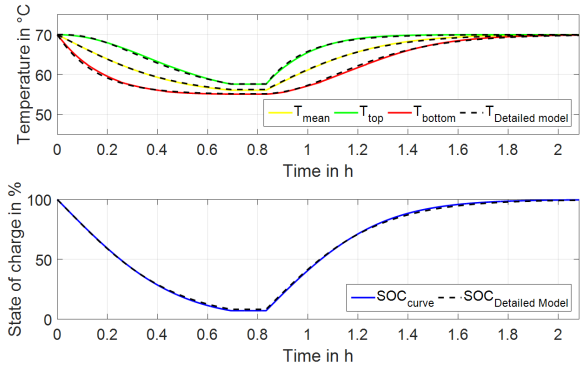

Figure 7: Loading and unloading of model with characteristic curves and detailed model.

As shown in figure 7, the generalized model has a good accordance with the detailed model. The comparison of the models is done for different tank volumes and temperature levels (e.g. 35/30 °C or 12/6 °C). The root-mean-square-deviation (RMSD) is used for evaluation and is calculated with equation (5).

$$RMSD = \sqrt{\left(\frac{\sum_{i=1}^{N} (\vartheta_{ref} - \vartheta_{ex})}{n} \right)}. \qquad (5)$$

To have a more general value for the evaluation the normalized root-mean-square-deviation (NRMSD) is used, calculated with equation (6). The results are presented in in table 4 and show that the deviations are below 2 %.

$$NRMSD = \left(\frac{RMSD}{(\vartheta_{ref,max} - \vartheta_{ref,min})} \right). \qquad (6)$$

Experiment and Simulation

To validate the developed models measurement data from a hardware test bench, which is shown in figure 8, is used.

Table 4: Normalized root-mean-square-deviation.

Storage Types	NRMSD ϑ_{mean}	NRMSD ϑ_{top}	NRMSD ϑ_{bottom}
70/55 °C (0.84 m^3)	0.9 %	1.5 %	1.7 %
70/55 °C (0.7 m^3)	0.8 %	1.4 %	1.5 %
70/55 °C (0.3 m^3)	0.5 %	0.9 %	0.9 %
35/30 °C (0.84 m^3)	0.9 %	1.5 %	1.7 %
12/6 °C (0.84 m^3)	0.9 %	1.4 %	1.7 %

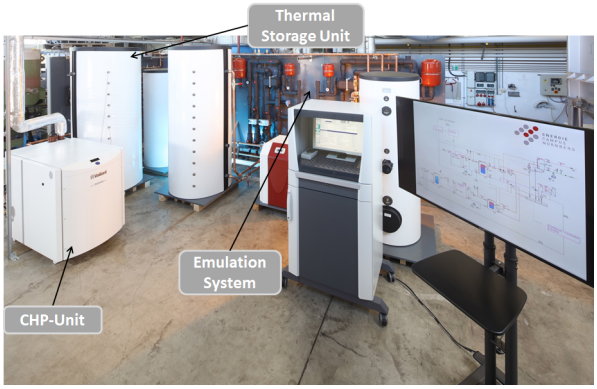

Figure 8: Hardware test bench for model validation.

The test bench consists of two heat generation units (HP-Unit and CHP-Unit), four TES and an emulation system, which allows the emulation of the heat demand of a virtual building. The test bench is coupled with the thermal building simulation environment TRNSYS. This enables the emulation of various building designs and the testing of the building devices under realistic conditions. For the validation of the storage models, a TES with a volume of 0.84 m^3 is used. The storage can be loaded by the installed CHP-Unit and unloaded by the emulation system. The examined storage unit is equipped with 11 temperature sensors distributed over the storage height. This allows a detailed evaluation of the temperature distribution during the loading and unloading process. Figure 9 shows the temperature profile of the storage during the loading. In addition, the corresponding inlet temperature and mass flow rate is presented.

During loading the mass flow rate, which enters the storage unit at the top layer is not constant. This is caused by the internal control of the CHP-Unit, which regulates the engine temperature. After some minutes, the mass flow rate stabilizes at approximately 10 l/min and the supply temperature stays at an almost constant value of 72 °C. At the end of the loading, the mass flow rate increases, what is also an result of the internal control. Like this the engine tempera-

ture can be kept nearly constant.

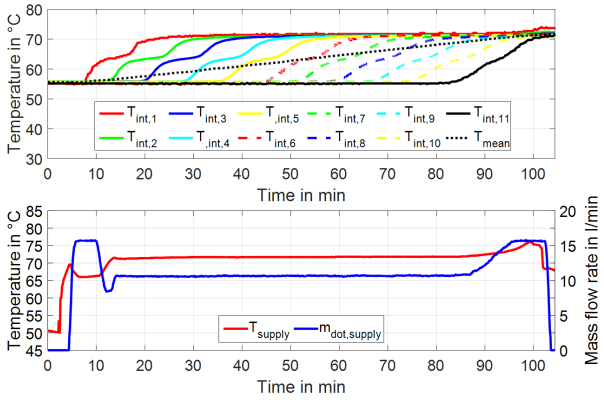

Figure 9: Loading of thermal buffer storage.

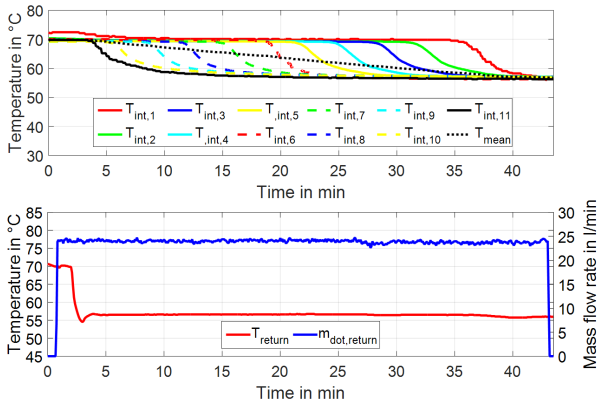

Figure 10: Unloading of thermal buffer storage.

During unloading, shown in figure 10, the volume flow rate, which enters the storage unit at the bottom layer, is kept constant at approx. 24 l/min and a return temperature of 56 °C.
In figure 9 and figure 10 the temperature stratification of the TES is getting apparent. At first the temperature of the layer at the top ($T_{int,1}$) shows a reaction to the incoming supply mass flow rate during loading. During unloading, it is the other way round, as the incoming water enters the storage at the bottom. In the simulation the detailed and generalized model, use the same mass flow rates and temperatures of the incoming fluids. Moreover, geometrical data from the manufacturers datasheet is used for the configuration of the models. The detailed and the generalized model work with only three temperature layers. For better comparison, the 11 sensors of the storage unit at the hardware test bench are aggregated and the mean values are assigned to the corresponding layer. Figure 11 shows the aggregation of the temperature sensors.

Discussion and result analysis

In this section, the simulation results of the two models are compared with the measurement data from the

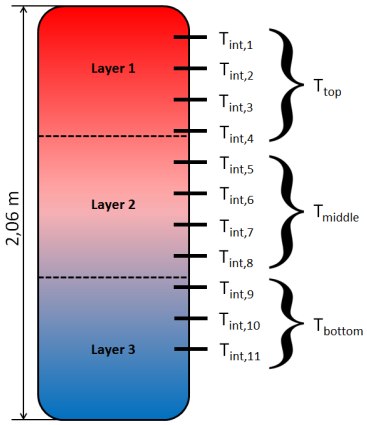

Figure 11: Aggregation of temperature sensors.

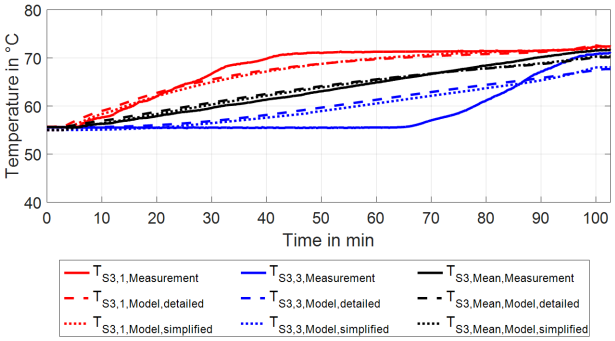

Figure 12: Loading of storage unit and storage models.

hardware test bench. The following figures (Figure 12 and 13) show the loading and unloading of the storage unit. The figures include the measurement data as well as the results from the two simulation models. Also in this analysis, the normalized root-mean-square-deviation is used. The calculation is analogue to the equations (5) and (6), but in this case, the measurement data is used as a reference. The results for the loading process are shown in table 5.

Table 5: Normalized root-mean-square-deviation during loading.

Model Type	**NRMSD** ϑ_{mean}	**NRMSD** ϑ_{top}	**NRMSD** ϑ_{bottom}
Detailed Model	6.0 %	8.2 %	21.7 %
Generalized Model	4.6 %	8.1 %	18.5 %

Table 5 shows, that the deviations of the detailed and the generalized model compared to the measured values are very similar. During loading, the bottom layer shows the highest deviations. This is also visible in figure 12, where the simulated temperature at the bottom does not reach the same value as the measured temperature at the end of the measurement series.

The deviations for the unloading process are shown in table 6. For the mean temperature the deviations are very similar during loading and unloading. For the top and the bottom layer, the deviations show a contrary behaviour, if the loading and unloading process is compared. For the top layer the deviations are higher during unloading, for the bottom layer during loading. This is also visible in figure 13, where the top layer temperature of the simulation is approximate 2.5 K higher than the measured temperature at the end of the measurement series.

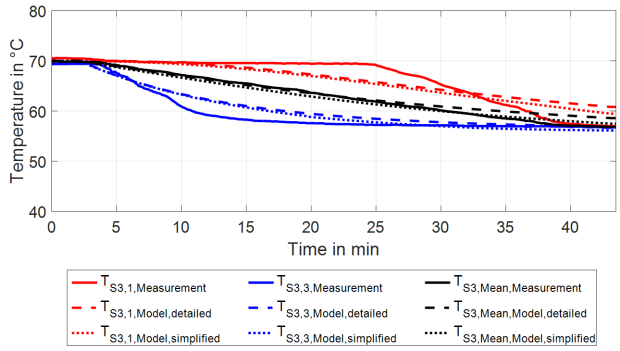

Figure 13: Unloading of storage unit and storage models.

Table 6: Normalized root-mean-square-deviation during unloading.

Model Type	**NRMSD** ϑ_{mean}	**NRMSD** ϑ_{top}	**NRMSD** ϑ_{bottom}
Detailed Model	7.0 %	15.5 %	11.6 %
Generalized Model	4.4 %	14.5 %	9.9 %

A possible reason for the higher deviations of the bottom or top layer temperature is the low number of simulated layers in the models. Here every layer is considered as a fully mixed segment, whereas the temperature within the real TES shows strong temperature stratification, which is visible in the figures 9 and 10.

Conclusion

This paper presents a generalization approach of a model for thermal buffer storages. Therefore, a detailed model is developed and used for the derivation of a generalized model, working with characteristic curves. The derived model shows a high concordance with the detailed model. It is also usable for different temperature levels as well as different storage geometries. For the validation of the models, measurement data from a hardware test bench is used. For the mean temperature of the storage, the deviation between simulated and measured values shows relatively low deviations with approx. 5 % during loading and unloading. For the top and the bottom layer, the deviation is higher and varies between 8 % and 22 %. A possible reason for the high deviation in the top and the bottom layer is the low number of layers during the simulation. The models work with three layers, which are assumed to be fully mixed and isotherm. In further research work, it is necessary to analyse, whether the deviations can be reduced with a higher number of simulated temperature layers.

Acknowledgements

This research has been performed as part of the Energie Campus Nuremberg under the project *SENSIBLE – Storage enabled sustainable energy for buildings and communities* funded by the European Union's Horizon research and innovation programme under grant agreement no. 645963.

Nomenclature

CHP-Unit	-	*Combined heat ant power unit*
HP-Unit	-	*Heat pump unit*
NRMSD	-	*Normalized-root-mean-square-deviation*
RMSD	-	*Root-mean-square-deviation*
SOC	-	*State of charge*
TES	-	*Thermal energy storage*

References

Arteconi, A., N. Hewitt, and F. Polonara (2013). Domestic demand-side management (DSM): Role of heat pumps and thermal energy storage (TES) systems. *Applied Thermal Engineering 51*, 155–165.

Becker, R. (2006). *Optimierung thermischer Systeme in dezentralen Energieversorgungsanlagen*. Ph. D. thesis, TU Dortmund University.

Dassault Systemes (2016). Dymola. Version 2016.

Math Works (2015). MATLAB. Version R2015a.

REN21 (2016). Renewables 2016 - global status report. Technical report, REN21 Community.

Solar Energy Laboratory (2012). TRNSYS. Version 17.01.

Thermal Energy System Specialists (2012). TESSLibs. Version 17.1.

TLK Thermo GmbH (2016). TIL Media. Version 3.4.0.

Widmann, C., D. Loedige, A. Toradmal, and B. Thomas (2017). Enabling CHP units for electricity production on demand by smart management of the thermal energy storage. *Applied Thermal Engineering 114*, 1487–1497.